

# Nonlinear optics of III-V semiconductors in the terahertz regime: an ab-initio study

Eric Roman,<sup>1</sup> Jonathan R. Yates,<sup>1,2</sup> Marek Veithen,<sup>3</sup> David Vanderbilt,<sup>4</sup> and Ivo Souza<sup>1,2</sup>

<sup>1</sup>*Department of Physics, University of California, Berkeley, CA 94720*

<sup>2</sup>*Materials Science Division, Lawrence Berkeley National Laboratory, Berkeley, CA 94720*

<sup>3</sup>*Département de Physique, Université de Liège, B-5, B-4000 Sart-Tilman, Belgium*

<sup>4</sup>*Department of Physics and Astronomy, Rutgers University, Piscataway, New Jersey 08854-8019*

(Dated: December 19, 2021)

We compute from first principles the infrared dispersion of the nonlinear susceptibility  $\chi^{(2)}$  in zincblende semiconductors. At terahertz frequencies the nonlinear susceptibility depends not only on the purely electronic response  $\chi_{\infty}^{(2)}$ , but also on three other parameters  $C_1$ ,  $C_2$  and  $C_3$  describing the contributions from ionic motion. They relate to the TO Raman polarizability, the second-order displacement-induced dielectric polarization, and the third-order lattice potential. Contrary to previous theory, we find that mechanical anharmonicity ( $C_3$ ) dominates over electrical anharmonicity ( $C_2$ ), which is consistent with recent experiments on GaAs. We predict that the sharp minimum in the intensity of second-harmonic generation recently observed for GaAs between  $\omega_{\text{TO}}/2$  and  $\omega_{\text{TO}}$  does not occur for several other III-V compounds.

PACS numbers: 78.30.Fs, 71.36.+c, 78.20.Jq, 42.65.An

## I. INTRODUCTION

The nonlinear optical properties of materials in the visible and near-infrared (IR) have been extensively studied since the development of the laser. Except for a few pioneering efforts,<sup>1,2</sup> the far-IR region of the spectrum has remained largely unexplored. This state of affairs, a consequence of the lack of tunable and intense laser sources and sensitive detectors in the terahertz range, is starting to change, thanks to advances in instrumentation.<sup>3,4</sup> More accurate measurements of the nonlinear susceptibilities at terahertz frequencies are beginning to appear,<sup>5</sup> calling for quantitative theoretical modeling.

The first nonlinear susceptibility  $\chi^{(2)}(\omega_3 = \omega_1 + \omega_2; \omega_1, \omega_2)$ , which is nonzero in acentric crystals, displays strong dispersion when the frequencies involved are near a zone-center transverse optical phonon frequency  $\omega_{\text{TO}}$ . This behavior was first observed by Faust and Henry<sup>1</sup> (see also Refs. 6 and 7) in GaP for the case of mixing between visible and far-IR radiation ( $\omega_1, \omega_1 + \omega_2 > \omega_{\text{TO}} > \omega_2$ ); they showed that the dispersion of this process depends on the linear electro-optic susceptibility  $\chi_{\text{eo}}^{(2)}$ . Another early set of experiments<sup>8,9</sup> investigated frequency mixing in the microwave range below the lattice resonances ( $\omega_1, \omega_2, \omega_1 + \omega_2 < \omega_{\text{TO}}$ ). For the two zincblende compounds studied, GaAs and GaP, it was found<sup>9</sup> that the sign of the microwave coefficient  $\chi_{\text{mw}}^{(2)}$  (the static nonlinear susceptibility) was opposite to that of the “high-frequency” coefficient  $\chi_{\infty}^{(2)}$  describing second-harmonic generation (SHG) and frequency mixing in the transparency region of the crystal ( $\omega_{\text{TO}} < \omega_1, \omega_2, \omega_1 + \omega_2 < E_g/\hbar$ ). Mayer and Keilmann<sup>2</sup> later studied the dispersion of the SHG coefficient  $\chi_{\text{SHG}}^{(2)}(\omega) = \chi^{(2)}(2\omega; \omega, \omega)$  of GaAs and LiTaO<sub>3</sub> over a limited frequency range (0.6 to 1.7 THz).

The present work was motivated by the recent experiments of Dekorsy *et al.* on SHG in GaAs.<sup>5</sup> Using a tun-

able free-electron laser they measured the dispersion of  $\chi_{\text{SHG}}^{(2)}$  from 4 to 6 THz, observing a strong resonant enhancement at 4.5 THz, close to  $\omega_{\text{TO}}/2 = 4.1$  THz as expected, followed by a sharp dip in the power output. Although they were unable to determine unambiguously the frequency  $\omega_0$  at which  $\chi_{\text{SHG}}^{(2)}$  vanishes, a lower bound of 5.3 THz was established. By fitting the location of the minimum in SHG power to an expression derived by Flytzanis,<sup>10</sup> they obtained new parameters for GaAs.

Flytzanis’s expression is given below [Eq. (1)]. Using an effective-bond model, he obtained numerical estimates for its parameters. These have been used as a guide for interpreting subsequent experiments,<sup>2,5</sup> in spite of their questionable reliability. For instance, the model predicts the wrong sign for the Born effective charge and the Raman polarizability, two of the material parameters at play. In this work we re-examine this problem using first-principles density-functional techniques.

The paper is organized as follows. In Sec. II we discuss the formalism describing the IR dispersion of  $\chi^{(2)}$ . The computational approach is explained in Sec. III. In Sec. IV we present and discuss results for several III-V semiconductors, GaAs, GaP, AlP, AlAs, and AlSb. Finally, in Sec. V we summarize our findings. Additional discussion of the computational methods is given in two Appendices.

## II. FORMALISM

In this work we limit ourselves to the zincblende structure adopted by III-V semiconductors, the simplest crystal structure where a non-vanishing  $\chi^{(2)}$  is allowed by symmetry. In zincblende there is a single TO mode, and third-rank tensors such as  $\chi^{(2)}$  have only one independent component  $\chi_{xyz}^{(2)}$ . The dispersion of  $\chi^{(2)}$  below the electronic resonances and above the elastic resonances of the medium is given by the following expression, obtained by

Flytzanis:<sup>10</sup>

$$\chi^{(2)}(\omega_1 + \omega_2; \omega_1, \omega_2) = \chi_\infty^{(2)} \Lambda(\omega_1, \omega_2), \quad (1)$$

where

$$\begin{aligned} \Lambda(\omega_1, \omega_2) = & 1 + C_1 \left( \frac{1}{D(\omega_1)} + \frac{1}{D(\omega_2)} + \frac{1}{D(\omega_1 + \omega_2)} \right) \\ & + C_2 \left( \frac{1}{D(\omega_1)D(\omega_2)} + \frac{1}{D(\omega_2)D(\omega_1 + \omega_2)} \right. \\ & \quad \left. + \frac{1}{D(\omega_1 + \omega_2)D(\omega_1)} \right) \\ & + C_3 \left( \frac{1}{D(\omega_1)D(\omega_2)D(\omega_1 + \omega_2)} \right) \end{aligned} \quad (2)$$

and  $D(\omega) = 1 - \omega^2/\omega_{\text{TO}}^2 - i\gamma\omega/\omega_{\text{TO}}^2$  is the resonance denominator with phonon damping. This expression can be derived under rather general conditions,<sup>11</sup> and is independent of the details of the microscopic forces, the only assumption being that the mode is weakly damped ( $\gamma \ll \omega_{\text{TO}}$ ).

The dispersion depends on three dimensionless coefficients,

$$C_1 = \frac{\alpha_{\text{TO}}}{2v\chi_\infty^{(2)}} \left( \frac{Z^*}{M\omega_{\text{TO}}^2} \right) \quad (3)$$

(known as the Faust-Henry coefficient),

$$C_2 = \frac{\mu^{(2)}}{2v\chi_\infty^{(2)}} \left( \frac{Z^*}{M\omega_{\text{TO}}^2} \right)^2, \quad (4)$$

and

$$C_3 = -\frac{\phi^{(3)}}{2v\chi_\infty^{(2)}} \left( \frac{Z^*}{M\omega_{\text{TO}}^2} \right)^3. \quad (5)$$

Here  $v$  is the volume of the primitive cell,  $M$  is the reduced mass, and the remaining quantities are discussed below. Unlike the second-rank tensor properties, the signs of the  $C_i$ 's remain unchanged if we reverse the definition of the positive [111] direction. We adopt the convention that it points from the cation to the closest anion.<sup>12,13</sup>

Having obtained the above model-independent expression for the IR dispersion of  $\chi^{(2)}$ , Flytzanis then proceeded to estimate the values of the coefficients  $C_1$ ,  $C_2$ , and  $C_3$  for several III-V compounds, using an effective-bond model.<sup>10</sup> We will now describe how to compute them from first-principles. Except for the damping parameter  $\gamma$  (which we do not calculate), the quantities entering Eqs. (1–5) are conveniently evaluated as derivatives of forces or macroscopic polarization with respect to macroscopic electric fields or displacements (forces under finite fields are readily available via the Hellmann-Feynman theorem<sup>14</sup>). In what follows  $\mathbf{F}$  represents the force on the cation,  $\mathbf{P}$  is the macroscopic polarization,  $\mathcal{E}$  is a macroscopic electric field, and  $\mathbf{u} = \mathbf{u}_{\text{III}} - \mathbf{u}_{\text{V}}$  is the

relative displacement between the cation (group III) and anion (group V) sublattices away from their equilibrium positions. Two of the quantities in Eqs. (1–5) are first derivatives: the cation Born effective charge

$$Z^* = v \left. \frac{\partial P_x}{\partial u_x} \right|_{\mathbf{E}=0} = \left. \frac{\partial F_x}{\partial \mathcal{E}_x} \right|_{\mathbf{u}=0}, \quad (6)$$

and the zone-center TO phonon frequency

$$\omega_{\text{TO}}^2 = -\frac{1}{M} \left. \frac{\partial F_x}{\partial u_x} \right|_{\mathcal{E}=0}. \quad (7)$$

The remaining four are second derivatives: the non-resonant electronic (“high-frequency”) quadratic susceptibility

$$\chi_\infty^{(2)} = \frac{1}{2} \left. \frac{\partial^2 P_x}{\partial \mathcal{E}_z \partial \mathcal{E}_y} \right|_{\mathbf{u}=0}, \quad (8)$$

the non-resonant TO Raman polarizability per primitive cell<sup>42</sup>

$$\alpha_{\text{TO}} = v \left. \frac{\partial [\chi_\infty^{(1)}]_{xy}}{\partial u_z} \right|_{\mathcal{E}=0} = \left. \frac{\partial^2 F_z}{\partial \mathcal{E}_x \partial \mathcal{E}_y} \right|_{\mathbf{u}=0}, \quad (9)$$

the second-order dipole moment or “electrical anharmonicity”

$$\mu^{(2)} = v \left. \frac{\partial^2 P_x}{\partial u_z \partial u_y} \right|_{\mathcal{E}=0}, \quad (10)$$

and the third-order lattice potential or “mechanical anharmonicity”

$$\phi^{(3)} = -\left. \frac{\partial^2 F_x}{\partial u_z \partial u_y} \right|_{\mathcal{E}=0}. \quad (11)$$

Note that in Eq. (9) the Raman tensor was recast as a second-order field-induced force.<sup>15,16</sup>

It will be useful to consider Eq. (1) in the three limiting cases discussed in the Introduction. In the high-frequency limit it reduces to the purely electronic coefficient  $\chi_\infty^{(2)}$ ; for  $\omega_1, \omega_1 + \omega_2 > \omega_{\text{TO}} > \omega_2$  it becomes the unclamped-ion, strain-free electro-optic coefficient,

$$\chi_{\text{eo}}^{(2)} = \chi_\infty^{(2)} (1 + C_1); \quad (12)$$

and finally for  $\omega_1, \omega_2, \omega_1 + \omega_2 < \omega_{\text{TO}}$  it describes the strain-free static (microwave) nonlinear susceptibility, which involves all three coefficients,

$$\chi_{\text{mw}}^{(2)} = \chi_\infty^{(2)} (1 + 3C_1 + 3C_2 + C_3). \quad (13)$$

### III. COMPUTATIONAL APPROACH

The calculations are done using **ABINIT**,<sup>17</sup> a plane-wave pseudopotential density-functional code, using both

the local-density approximation (LDA) and a generalized gradient approximation<sup>18</sup> (GGA). In order to better assess the sensitivity of the nonlinear optical properties to the approximate density functional used, all calculations are performed at the same (experimental) lattice constants. Norm-conserving Troullier-Martins pseudopotentials<sup>19</sup> are used for all materials, and for Ga the  $d$ -electrons are included in the valence. We used a cutoff energy of 30 Ha for the aluminum compounds, and 45 Ha for the gallium compounds.

For finite systems such as molecules, *ab-initio* calculations of  $\chi^{(2)}$  below the electronic resonances (including contributions from ionic motion<sup>20</sup>) are performed routinely. Similar calculations for bulk solids have become feasible only recently, thanks to a series of developments, starting with the Berry-phase theory of polarization,<sup>21</sup> which provides a means of evaluating the electronic contribution to the macroscopic polarization  $\mathbf{P}$  as a bulk quantity (for a review, see Ref. 22). In Ref. 23 a density-functional perturbation method was developed for computing nonlinear (electronic, electro-optic, and nonresonant Raman) susceptibilities using the Berry-phase formalism to treat the electric field perturbation. Here we use a closely-related approach where the derivatives are evaluated by finite differences rather than analytically, using the method of Ref. 14 to handle finite electric fields. The appeal of this method lies in its simplicity: once implemented, no extra coding is required to compute a different higher-order or mixed derivative, or to switch from, e.g., LDA to GGA.

In our calculations we apply the finite perturbation ( $\mathbf{u}$  or  $\mathcal{E}$ ) along [111], and monitor the response ( $\mathbf{P}$  or  $\mathbf{F}$ ) along the same direction. That is, we let  $\mathbf{u} = \delta a(\hat{\mathbf{x}} + \hat{\mathbf{y}} + \hat{\mathbf{z}})$ , where  $a$  is the lattice constant and the cation and anion sublattices are brought closer together when  $\delta > 0$ ;  $\mathcal{E} = \varepsilon E_0(\hat{\mathbf{x}} + \hat{\mathbf{y}} + \hat{\mathbf{z}})$ , where  $E_0 = e/(4\pi\epsilon_0 a_0^2)$ ;  $\mathbf{F} = f(\hat{\mathbf{x}} + \hat{\mathbf{y}} + \hat{\mathbf{z}})$ ; and  $\Delta\mathbf{P} = p(\hat{\mathbf{x}} + \hat{\mathbf{y}} + \hat{\mathbf{z}})$ . Eqs. (6–11) then become

$$Z^* = \frac{a^2}{4} \frac{\partial p}{\partial \delta} = \frac{\partial f}{\partial \varepsilon}, \quad (14)$$

$$\omega_{\text{TO}}^2 = -\frac{1}{aM} \frac{\partial f}{\partial \delta}, \quad (15)$$

$$\chi_{\infty}^{(2)} = \frac{1}{4} \frac{\partial^2 p}{\partial \varepsilon^2}, \quad (16)$$

$$\alpha_{\text{TO}} = \frac{1}{2} \frac{\partial^2 f}{\partial \varepsilon^2}, \quad (17)$$

$$\mu^{(2)} = \frac{a}{8} \frac{\partial^2 p}{\partial \delta^2}, \quad (18)$$

and

$$\phi^{(3)} = -\frac{1}{2a^2} \frac{\partial^2 f}{\partial \delta^2}. \quad (19)$$

The parameters are calculated from these expressions, and then inserted into Eqs. (3–5) to obtain the coefficients  $C_1$ ,  $C_2$ , and  $C_3$ . In Appendix A we describe a different approach whereby  $\chi_{\text{eo}}^{(2)}$  and  $\chi_{\text{mw}}^{(2)}$  are evaluated directly by finite differences in addition to  $\chi_{\infty}^{(2)}$ , and Eqs. (12) and (13) are then used to obtain  $C_1$  and  $3C_2 + C_3$ .

We have taken as the smallest increments  $\delta = 1 \times 10^{-3}$  and  $\varepsilon = 1 \times 10^{-4}$  for AlAs, AlP, GaP, and AlSb. In the case of GaAs a smaller field step of  $\varepsilon = 3 \times 10^{-5}$  was used. This was needed in order to stay below the  $k$ -mesh dependent critical field above which the electric enthalpy functional loses its minima.<sup>14</sup> Because of its smaller band gap, the critical field is lower for GaAs than for the other compounds.

For the derivatives we use Richardson's extrapolation to estimate the limit  $h \rightarrow 0$  from calculations with two different step sizes:

$$f^{(n)}(x) = \frac{4}{3}D^{(n)}(x, h) - \frac{1}{3}D^{(n)}(x, 2h) + \mathcal{O}(h^4), \quad (20)$$

where  $D^{(1)}$  is given by the centered finite difference expression

$$D^{(1)}(x, h) \equiv \frac{f(x+h) - f(x-h)}{2h} = f'(x) + \mathcal{O}(h^2), \quad (21)$$

and  $D^{(2)}$  is given by

$$\begin{aligned} D^{(2)}(x, h) &\equiv \frac{f(x+h) + f(x-h) - 2f(x)}{h^2} \\ &= f''(x) + \mathcal{O}(h^2). \end{aligned} \quad (22)$$

In order to speed up the convergence of polarization-dependent quantities with respect to the  $k$ -point sampling, we use a similar extrapolation for the discretized Berry-phase formula, as described in Appendix B. All the values quoted in the tables were calculated on a  $16 \times 16 \times 16$   $k$ -point mesh, except in the case of GaAs which, for reasons discussed in that Appendix, demanded a denser mesh.

## IV. RESULTS FOR III-V SEMICONDUCTORS

### A. Microscopic parameters

We have systematically computed the values of all six parameters (6–11), using the methods summarized above, for five III-V compounds. The results are collected in Table I, and we will begin by discussing the comparison with the model theory of Flytzanis, and then pass to the discussion of the experimental values.

Table I shows striking differences between the first-principles results and Flytzanis's model calculations: (i) While both levels of theory produce the same sign for  $\chi_{\infty}^{(2)}$ , they disagree on the signs of  $Z^*$ ,  $\alpha_{\text{TO}}$ ,  $\mu^{(2)}$ , and

TABLE I: Parameters that determine the nonlinear susceptibility of zincblende compounds in the infrared range, grouped into first- and second-derivative quantities [Eqs. (6–11)]. Rows labelled “Model” pertain to the empirical-model calculations of Flytzanis:  $\chi_\infty^{(2)}$  is taken from Ref. 24, the remaining values from Ref. 10.

		First derivative		Second derivative			
		$Z^*$	$\omega_{\text{TO}}$ (THz)	$\chi_{\infty}^{(2)}$ (pm/V)	$\alpha_{\text{TO}}$ (Å <sup>2</sup> )	$\mu^{(2)}$ (nC/m)	$\phi^{(3)}$ (TJ/m <sup>3</sup> )
GaAs	LDA	2.05	8.0	472	−54	−1.89	4.29
	GGA	2.05	8.3	337	−34	−1.67	5.10
	Model			127	84	5.90	−1.2
	Expt.	2.2 <sup>a</sup>	8.0 <sup>a</sup>	170 <sup>b</sup>	−38 <sup>c</sup>		
GaP	LDA	2.10	10.6	131	−12.9	−1.50	4.82
	GGA	2.15	10.9	114	−9.8	−1.36	4.76
	Model	−2.0	11.5	93	43	7.77	−2.1
	Expt.	2.0 <sup>a</sup>	11.0 <sup>a</sup>	71 <sup>b</sup>	−20 <sup>c</sup>		
AlP	LDA	2.24	12.7	45	−5	0.28	4.64
	GGA	2.24	13.1	42	−5	0.24	4.32
	Expt.	2.28 <sup>a</sup>	13.2 <sup>d</sup>				
AlAs	LDA	2.14	10.4	79	−9	0.27	4.00
	GGA	2.11	10.8	73	−8	0.22	4.94
	Expt.	2.3 <sup>a</sup>	10.8 <sup>e</sup>				
AlSb	LDA	1.86	9.2	205	−19	−0.09	3.09
	GGA	1.79	9.5	187	−18	−0.12	3.34
	Model	−1.6	9.8	47	77	8.34	−1.5
	Expt.	1.9 <sup>a</sup>	9.6 <sup>a</sup>	153 <sup>b</sup>			

<sup>a</sup>Quoted in Ref. 25.

<sup>b</sup>Ref. 26.

<sup>c</sup>Ref. 27.

<sup>d</sup>Quoted in Ref. 28.

<sup>e</sup>Quoted in Ref. 29.

$\phi^{(3)}$ . (ii) We find that the magnitude of  $\mu^{(2)}$  ( $\phi^{(3)}$ ) is significantly smaller (larger) than Flytzanis predicts.

Born charges and phonon frequencies are routinely computed from first-principles, and they tend to compare favorably with experiment,<sup>29</sup> as evidenced in Table I. Dielectric susceptibilities and Raman polarizabilities are more problematic. For example, it is well-known that density-functional theory tends to overestimate the dielectric constant. This also seems to be generally the case for the nonlinear susceptibility  $\chi_\infty^{(2)}$ .<sup>30,31</sup> The problem here is compounded by the fact that the experimental determination of this quantity is also problematic, with the values reported in the literature displaying a very large dispersion.<sup>27</sup> We have opted for quoting the recommended values from Landolt-Börnstein.<sup>26</sup> Inspection of Table I suggests that our first-principles values are too large by roughly a factor of two, which however is comparable with the uncertainty in the experimental determination. Measurements of the absolute Raman polarizability are also difficult, and few values are reported in the literature. Our result that  $\alpha_{\text{TO}} < 0$  means that the bond polarizability along [111] increases with increasing bond length around the equilibrium length of the bond. This is in agreement with the measured sign in GaAs,<sup>13</sup> but in disagreement with the model calculations

of Flytzanis.<sup>10,32</sup>

## B. Lattice-induced contributions to $\chi^{(2)}$

From the calculated parameters in Table I we obtained, using Eqs. (3–5), the various lattice-induced contributions to  $\chi^{(2)}$ , collected in Table II. We find that the Faust-Henry coefficients  $C_1$  are roughly a factor of two smaller than the experimental values, consistent with the overestimation of  $\chi_\infty^{(2)}$  in Eq. (3) discussed above. The mechanical anharmonicity coefficient  $C_3$  is, in all cases, significantly larger in magnitude than  $C_2$  (electrical anharmonicity). This is the opposite conclusion from Refs. 10 and 33. We remark that although the correct signs for  $C_1$  and  $C_3$  were obtained therein, this resulted from a cancellation of errors in the signs of  $Z^*$ ,  $\alpha_{\text{TO}}$ , and  $\phi^{(3)}$  in Eqs. (3) and (5). No such cancellation occurs in  $C_2$ , and indeed for the three compounds studied both in the present work and in Ref. 10 (AlSb, GaP and GaAs), there is a disagreement in the predicted sign for this quantity.

While the coefficient  $C_1$  can be measured in various ways (electro-optic effect, frequency mixing,<sup>1</sup> and relative Raman scattering efficiencies from LO and TO phonons<sup>34,35</sup>) with fairly consistent results, it is difficult to disentangle the values of  $C_2$  and  $C_3$  from experiments. The more readily accessible quantity is the combination  $3C_2 + C_3$ : it follows from Eqs. (12) and (13) that

$$3C_2 + C_3 = 2 + \frac{\chi_{\text{mw}}^{(2)} - 3\chi_{\text{eo}}^{(2)}}{\chi_\infty^{(2)}}, \quad (23)$$

where all the quantities on the right-hand-side are directly measurable. Flytzanis found  $C_2 > 0$  and  $C_3 < 0$  for all the III-V compounds he investigated. Under those circumstances, the measured sign of  $3C_2 + C_3$  indicates which anharmonic contribution (electrical or mechanical) is dominant in a given material. We find, however, that the sign of  $C_2$  is not the same for all III-V compounds, which invalidates such an analysis.

Interestingly, our calculated  $3C_2 + C_3$  disagree in sign with the values inferred from experiment<sup>8,9</sup> (see Table III). It is apparent from Eq. (23) that the sign of  $3C_2 + C_3$  is rather sensitive to not only the signs, but also the relative magnitudes of  $\chi_{\text{eo}}^{(2)}$  and  $\chi_{\text{mw}}^{(2)}$ . While the signs of our calculated  $\chi_{\text{mw}}^{(2)}$  and  $\chi_{\text{eo}}^{(2)}$  agree with experiment (see Table III) there is a significant discrepancy regarding their magnitudes. The well-known limitations of density-functional theory in reproducing dielectric properties, such as the optical gap (underestimated) and the dielectric constant (overestimated) may be of concern in this regard. We note however that a possible error in the magnitude of  $\chi_\infty^{(2)}$  will not affect the sign of  $3C_2 + C_3$ , while  $\phi^{(3)}$ ,  $Z^*$ , and  $\mu^{(2)}$ , the remaining parameters entering  $C_2$  and  $C_3$ , are expected to be reasonably accurate within density functional theory, which typically describe rather well lattice-dynamical and zero-field polarization properties (e.g., Born charges) of III-V semiconductors.<sup>29</sup>

TABLE II: Lattice-induced contributions to the nonlinear susceptibility of zincblende compounds [Eqs. (3–5)]. Rows labelled “Model” pertain to the empirical-model calculations of Flytzanis.

		$C_1$	$C_2$	$C_3$
AlP	LDA	−0.38	0.05	−1.82
	GGA	−0.37	0.04	−1.78
AlAs	LDA	−0.37	0.03	−0.91
	GGA	−0.34	0.02	−0.82
AlSb	LDA	−0.25	−0.00	−0.22
	GGA	−0.23	−0.00	−0.18
	Model	−1.97	0.35	−0.11
GaP	LDA	−0.27	−0.04	−0.53
	GGA	−0.28	−0.07	−0.56
	Model	−0.37	0.11	−0.05
	Expt.	−0.53 <sup>a</sup>		
	Expt.	−0.75 <sup>a</sup>		
GaAs	LDA	−0.35	−0.02	−0.12
	GGA	−0.29	−0.03	−0.15
	Model	−0.83	0.14	−0.07
	Expt.	−0.51 <sup>a</sup>		
	Expt.	−0.59 <sup>b</sup>		
	Expt.	−0.68 <sup>a</sup>		
	Expt.	−0.48 <sup>c</sup>		

<sup>a</sup>Quoted in Ref. 10.

<sup>b</sup>Ref. 34.

<sup>c</sup>Ref. 36.

Hence our prediction for the sign for  $3C_2 + C_3$  should be sound. In view of the discrepancy with experiment, it would be useful to have careful measurements of the relative magnitudes of  $\chi_{\text{mw}}^{(2)}$  and  $\chi_{\text{eo}}^{(2)}$ , but we are not aware of any other work along these lines besides the pioneering investigations of Boyd *et al.*<sup>8,9</sup>

A convenient measure of the relative importance of the two lattice-anharmonicity mechanisms is the ratio  $C_2/C_3$ , also included in Table III. We expect reasonably accurate *ab-initio* results for this quantity, since it is independent of  $\chi_{\infty}^{(2)}$ , the “weak link” in the calculation. Our values clearly cannot be reconciled with those of Flytzanis. In the next section we will discuss what this implies for the interpretation of the recent experiment of Dekorsy *et al.*,<sup>5</sup> which attempted to obtain values for the parameters  $C_2$  and  $C_3$  separately for the first time.

### C. Zero-crossings of $\chi_{\text{SHG}}^{(2)}$ in the terahertz range

The quantity  $|\chi_{\text{SHG}}^{(2)}(\omega)|$  is displayed in Fig. 1 for GaAs. The dashed line in the upper panel correspond to a sensible choice of parameters assembled from the experimental and theoretical investigations from the 1960’s and 1970’s (these will be referred to as “old parameters”). In between the expected strong resonant enhancements at  $\omega_{\text{TO}}/2$  and  $\omega_{\text{TO}}$ , there are two dips, at 5.1 and 7.4 THz, the first more pronounced than the second. They result from sign reversals of  $\text{Re}\chi_{\text{SHG}}^{(2)}(\omega)$  in Eq. (1). If SHG is

TABLE III: Third and fourth columns: parameters  $C_2$  and  $C_3$  combined in a way that relates more directly to experiments. Fifth and sixth columns: electro-optic and microwave nonlinear susceptibilities of Eqs. (12) and (13) (in pm/V). Rows labelled “Model” pertain to the empirical-model calculations of Flytzanis.

		$3C_2 + C_3$	$C_2/C_3$	$\chi_{\text{eo}}^{(2)}$	$\chi_{\text{mw}}^{(2)}$
AlP	LDA	−1.68	−0.026	28	−82
	GGA	−1.66	−0.022	26	−74
AlAs	LDA	−0.83	−0.028	50	−75
	GGA	−0.77	−0.023	48	−58
AlSb	LDA	−0.23	0.012	154	6
	GGA	−0.19	0.017	145	25
	Model	0.93	−3.33		
GaP	LDA	−0.71	0.146	88	−90
	GGA	−0.78	0.128	82	−69
	Model	0.27	−2.22		
	Expt.	0.28 <sup>a</sup>		20 <sup>a</sup>	−24 <sup>a</sup>
GaAs	LDA	−0.19	0.203	309	−107
	GGA	−0.22	0.175	240	−30
	Model	0.35	−1.96		
	Expt.	0.39 <sup>a</sup>		43 <sup>a</sup>	−51 <sup>a</sup>

<sup>a</sup>Refs. 8,9.

observed over a frequency range containing the first zero crossing, its frequency  $\omega_0$  can be detected as a sharp dip in the second harmonic power. If, furthermore,  $3C_2 + C_3$  is known from separate measurements of  $\chi_{\infty}^{(2)}$ ,  $\chi_{\text{eo}}^{(2)}$  and  $\chi_{\text{mw}}^{(2)}$ ,<sup>8,9</sup> the remaining free parameter in Eq. (1),  $C_2/C_3$ , can then be adjusted to fit the zero-crossing frequency. This was proposed in Ref. 2 as a way of determining  $C_2$  and  $C_3$  separately.

Dekorsy *et al.*<sup>5</sup> recently used a free-electron laser to measure the far-IR dispersion of the SHG power in GaAs from 4.4 to 5.6 THz. They observed the expected resonance close to  $\omega_{\text{TO}}/2$ , followed by a strong drop. Because of insufficient filtering of the fundamental signal in the detector above 5.6 THz, which masked the SHG signal, they were unable to locate precisely the zero crossing, and only a *lower bound* of 5.3 THz was established. Since this is slightly above the 5.1 THz predicted for  $\omega_0$  from the old parameters, they then discussed how the values of  $C_2$  and  $C_3$  had to be revised to increase  $\omega_0$  to 5.3 THz (the assumption being that the lower bound is reasonably close to the actual zero-crossing). They opted to leave  $3C_2 + C_3$  unchanged at 0.35 (the theoretical value from Ref. 10, which is fairly close to the experimental 0.39); a good fit, shown as a solid line in the upper panel of Fig. 1, was then obtained by changing  $C_2/C_3$  from −2.0 to about −1.23. This amounts to essentially doubling  $C_3$ , from −0.07 to −0.14, while changing  $C_2$  only slightly, from 0.14 to 0.16.

The dashed line in the lower panel of Fig. 1 shows the dispersion obtained with our *ab-initio* parameters. The zero-crossing frequency is raised significantly, to 6.2 THz. In order to assess the impact of the uncertainty in  $\chi_{\infty}^{(2)}$

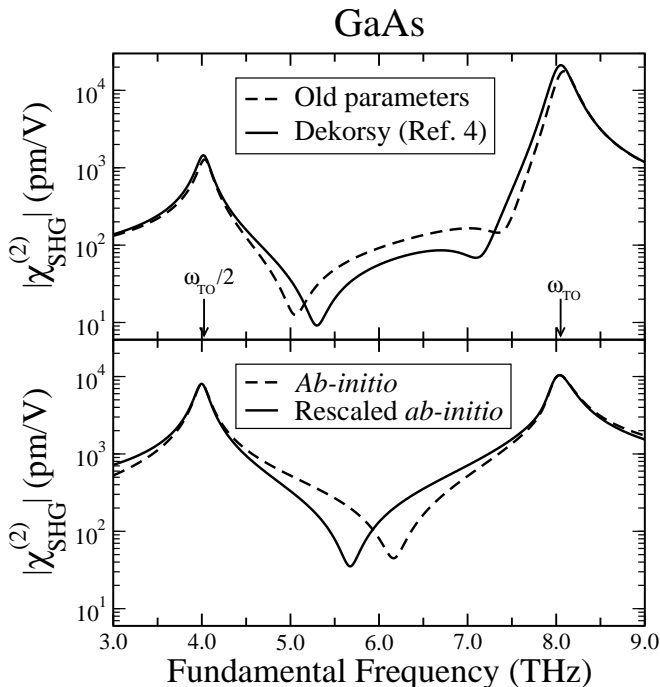


FIG. 1: Calculated IR dispersion of  $|\chi_{\text{SHG}}^{(2)}(\omega)|$  in GaAs, for different choices of the parameters in Eq. (1).  $(C_1, C_2, C_3) = (-0.59, 0.14, -0.07)$ ,  $(-0.59, 0.16, -0.13)$ ,  $(-0.35, -0.024, -0.12)$  and  $(-0.59, -0.041, -0.20)$  for the curves labeled ‘Old parameters,’ ‘Dekorsky,’ ‘*Ab-initio*,’ and ‘Rescaled *ab-initio*,’ respectively. Following Ref. 5, we set the damping parameter  $\gamma$  to 0.29 THz. The meaning of these parameter sets is explained in the text.

on the dispersion, we show as a solid line the curve that results from reducing  $\chi_{\infty}^{(2)}$  from 472 pm/V to 277 pm/V. This affects the  $C_i$ ’s according to Eqs. (3–5), and we have chosen the amount of rescaling so as to bring our value for  $C_1$  into agreement with the experimental number from Ref. 34,  $C_1 = -0.59$ . The zero-crossing frequency also changes, from 6.2 THz to 5.67 THz, only slightly above the measured lower bound of 5.3 THz. Clearly, different sets of values for  $C_2$  and  $C_3$  can lead to dispersions with very similar zero crossings (the solid lines in the two panels of Fig. 1), and thus both consistent with the experimental data, underscoring the need for reliable theoretical input. Interestingly, we find that for the other III-V compounds no zero crossing occurs for  $\omega_{\text{TO}}/2 < \omega < \omega_{\text{TO}}$ . This is illustrated in Fig. 2 for GaP.

## V. SUMMARY

We have carried out a detailed *ab-initio* investigation of the IR dispersion of the non-linear susceptibility  $\chi^{(2)}$  in III-V zincblende semiconductors. The results were compared with Flytzanis’s empirical model<sup>10</sup> and with experiment, with particular emphasis on the recent second-harmonic generation measurements carried out by Deko-

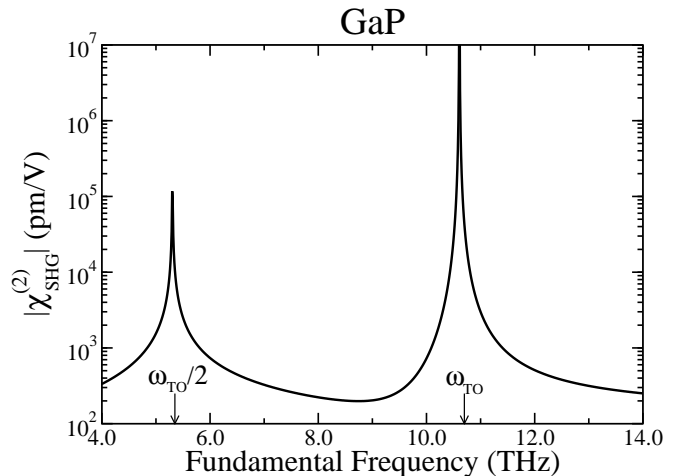


FIG. 2: Calculated IR dispersion of  $|\chi_{\text{SHG}}^{(2)}|$  in GaP, using the *ab-initio* parameters without damping ( $\gamma = 0$  THz). In contrast to GaAs (Fig. 1), no sharp dip is observed between the two maxima at  $\omega_{\text{TO}}/2$  and  $\omega_{\text{TO}}$ .

rsy *et al.*<sup>5</sup> These authors based the interpretation of their data on the parameters obtained in Ref. 10 from model calculations. By revising them somewhat, they were able to obtain a reasonable fit to the IR dispersion of  $\chi_{\text{SHG}}^{(2)}$ . Instead, we find a completely different set of parameters, which however is still consistent with experiment.

Our findings can be summarized as follows: (i) We provide theoretical support to the main qualitative conclusion of Ref. 5, that the ratio  $|C_2/C_3|$  between the contribution from second-order lattice dipole moment ( $C_2$ ) versus phonon interaction through the third-order lattice potential anharmonicity ( $C_3$ ) is smaller than previously thought. (ii) However, we find that this is a consequence of not only an increase in  $|C_3|$ ,<sup>5</sup> but also a significant decrease in  $|C_2|$ , with the result that the former dominates the latter ( $|C_2/C_3| \ll 1$ ). (iii) The sign of  $C_2$  is not constant throughout the III-V series, and for the two most-studied compounds (GaAs and GaP) it is negative, contrary to prior understanding. (iv) For all compounds except AlSb, we find that the sign of the microwave non-linear susceptibility  $\chi_{\text{mw}}^{(2)}$  is opposite to that of the optical ( $\chi_{\infty}^{(2)}$ ) and electro-optical ( $\chi_{\text{eo}}^{(2)}$ ) coefficients, in agreement with early experiments on GaAs and GaP.<sup>8,9</sup> However, our calculated negative sign for  $3C_2 + C_3$ , which is sensitive to the relative magnitudes of  $\chi_{\text{eo}}^{(2)}$  and  $\chi_{\text{mw}}^{(2)}$ , disagrees with those experiments. (v) The parameter fit to the IR dispersion of  $\chi_{\text{SHG}}^{(2)}$  relies on the occurrence of a sharp minimum in SHG power between  $\omega_{\text{TO}}/2$  and  $\omega_{\text{TO}}$ . The observed zero-crossing in GaAs is reproduced by our calculations, but is also consistent with an alternative set of parameters characterized by  $3C_2 + C_3 > 0$  and  $|C_2/C_3| > 1$ . For the other compounds considered, we find no zero-crossing.

## VI. ACKNOWLEDGMENTS

This work was supported by the Laboratory Directed Research and Development Program of Lawrence Berkeley National Laboratory under the Department of Energy Contract No. DE-AC02-05CH11231 and by NSF Grant DMR-0549198.

### APPENDIX A: A METHOD FOR THE DIRECT EVALUATION OF $C_1$ AND $3C_2 + C_3$

As discussed in the main text, by using Eqs. (12) and (13) one can obtain experimental values for  $C_1$  and  $3C_2 + C_3$  from separate measurements of  $\chi_\infty^{(2)}$ ,  $\chi_{eo}^{(2)}$ , and  $\chi_{mw}^{(2)}$ . In this Appendix we describe the computer-experiment analogs of such measurements.

We define “high-frequency” (optical) fields  $\mathcal{E}$  and “low-frequency” (static) fields  $\mathbf{E}$  as follows:<sup>23</sup> when an optical field  $\mathcal{E}$  is applied the ions are not allowed to move, so that the polarization response is purely electronic; in contrast, both ions and electrons respond to a static field  $\mathbf{E}$ , resulting in a total change in polarization that contains ionic as well as electronic contributions (but the cell is kept strain-free, since we are interested in frequencies above the elastic resonances of the medium). In Ref. 14 the high-frequency and static dielectric constants,  $\epsilon_\infty$  and  $\epsilon_0$ , were evaluated by finite differences as first derivatives with respect to  $\mathcal{E}$  and  $\mathbf{E}$ , respectively. Extending this to second order yields the high-frequency  $\chi_\infty^{(2)}$  and the low frequency (microwave)  $\chi_{mw}^{(2)}$ .

Evaluating the electro-optic  $\chi_{eo}^{(2)}$  requires combining a static and an optical field:

$$[\chi_{eo}^{(2)}]_{xyz} = \frac{1}{2} \frac{d}{dE_z} \left( \frac{\partial P_x}{\partial \mathcal{E}_y} \right) = \frac{1}{2} \frac{d}{dE_z} [\chi_\infty^{(1)}]_{xy}. \quad (\text{A1})$$

Here the action of the static field is described by a total derivative as a reminder that the polarization depends on a static field both explicitly and implicitly, through the atomic positions. Clearly the order of the (partial and total) derivatives matters. We can view their combined action as a conventional mixed derivative on an auxiliary function  $\tilde{\mathbf{P}}(\mathbf{E}, \mathcal{E})$  defined as follows: (i) apply a field  $\mathbf{E}$  and let both electrons and ions respond; (ii) add a field  $\mathcal{E}$ , let the electrons readjust under the total field  $\mathbf{E} + \mathcal{E}$  while keeping the ions fixed in the positions obtained in the first step.  $\tilde{\mathbf{P}}(\mathbf{E}, \mathcal{E})$  is defined as the polarization after step (ii). Then

$$\left. \frac{d}{dE_z} \left( \frac{\partial P_x}{\partial \mathcal{E}_y} \right) \right|_{\mathbf{E}=\mathcal{E}=0} = \frac{\partial^2 \tilde{P}_x}{\partial E_z \partial \mathcal{E}_y} = \frac{\partial^2 \tilde{P}_x}{\partial \mathcal{E}_y \partial E_z}. \quad (\text{A2})$$

As before, we apply small fields along [111]:  $\mathbf{E} = \epsilon(\hat{\mathbf{x}} + \hat{\mathbf{y}} + \hat{\mathbf{z}})$ , and  $\mathcal{E} = \epsilon(\hat{\mathbf{x}} + \hat{\mathbf{y}} + \hat{\mathbf{z}})$ . Then, defining  $\Delta \tilde{\mathbf{P}}(\mathbf{E}, \mathcal{E}) = \tilde{\mathbf{p}}(\epsilon, \epsilon)(\hat{\mathbf{x}} + \hat{\mathbf{y}} + \hat{\mathbf{z}})$ , we find

$$\chi_{eo}^{(2)} = \frac{1}{4} \frac{\partial^2 \tilde{p}}{\partial \epsilon \partial \epsilon}, \quad (\text{A3})$$

which we evaluate as

$$\begin{aligned} \frac{\partial^2 \tilde{p}}{\partial \epsilon \partial \epsilon} &= \frac{\tilde{p}(\epsilon, \epsilon) - \tilde{p}(\epsilon, -\epsilon) - \tilde{p}(-\epsilon, \epsilon) + \tilde{p}(-\epsilon, -\epsilon)}{4\epsilon\epsilon} \\ &+ \mathcal{O}(\epsilon^2, \epsilon^2). \end{aligned} \quad (\text{A4})$$

We found that a more stringent force tolerance for the atomic relaxations must be used when evaluating  $\chi_{mw}^{(2)}$  than when evaluating  $\chi_{eo}^{(2)}$ . This results from the fact that in the latter case the displacements are second-order in the field, whereas in the former they are first-order.<sup>37</sup> Well-converged values were obtained by using a force tolerance of  $10^{-7}$  Ha/bohr for  $\chi_{mw}^{(2)}$ , while for  $\chi_{eo}^{(2)}$   $10^{-5}$  Ha/bohr was sufficient.

The values for  $\chi_{eo}^{(2)}$  and  $\chi_{mw}^{(2)}$  obtained using this method agree to within 1 pm/V with the ones obtained from the separate calculation of  $C_1$ ,  $C_2$  and  $C_3$  described in Sec. III. This provides an internal consistency check of our calculations. Although it is somewhat more expensive and does not provide as much information (e.g., it does not produce separate values for  $C_2$  and  $C_3$ ), the method described in this Appendix provides a simple means of controlling the mechanical boundary conditions under applied fields. Although we only considered atomic displacements, the same strategy can be extended to strain deformations. In this way one can easily compute, for example, the clamped (strain-free) and unclamped (stress-free) electro-optic coefficients, or the static  $\chi^{(2)}$  including the strain response.<sup>37</sup>

### APPENDIX B: IMPROVING THE CONVERGENCE WITH RESPECT TO $k$ -POINT SAMPLING

Although total-energy ground state calculations for insulators converge exponentially fast with respect to  $k$ -point sampling, for finite-field calculations the convergence is considerably slower.<sup>38</sup> This results from the discretized Berry-phase (DBP) polarization expression (Eq. (B2) below) used in the electric enthalpy functional,<sup>14</sup> and as a consequence the second field-derivatives in Eqs. (8) and (9) also converge slowly. In order to alleviate this problem we used in our finite-field calculations a modified DBP expression for the polarization, Eq. (B4) below.

For notational simplicity we limit our discussion to the case of a single valence band in one dimension. The electronic polarization of a bulk insulator under periodic boundary conditions can be written, by analogy with the dipole moment of a molecule, as  $P_{el} = -e\langle x \rangle / L$ , where  $L$  is the length of the periodic box. The Berry-phase expression for  $\langle x \rangle$  is<sup>39</sup>

$$\langle x \rangle \simeq \frac{L}{2\pi} \text{Im} \ln \langle \Psi | e^{i \frac{2\pi x}{L}} | \Psi \rangle, \quad (\text{B1})$$

where  $\Psi$  is a many-body insulating wavefunction. For a finite system in a supercell, evaluating the dipole

moment with this expression amounts to replacing the non-periodic operator  $x$  with the periodic operator  $(L/2\pi)\sin(2\pi x/L)$ .<sup>40</sup> The difference between the two near the origin, where the molecule is located, is of order  $1/L^2$ . Using for  $\Psi$  a Slater determinant of single-particle Bloch states, we recover from this expression the King-Smith-Vanderbilt DBP expression for the polarization of a band insulator:<sup>39</sup>

$$P_{\text{el}} = -\frac{e}{2\pi} \text{Im} \ln \prod_{s=0}^{N-1} \det S(k_s, k_{s+1}) + \mathcal{O}(1/L^2), \quad (\text{B2})$$

where  $S(k_s, k_{s+1}) = \langle u_{k_s} | u_{k_{s+1}} \rangle$ . An alternative expression for  $\langle x \rangle$  is

$$\langle x \rangle \simeq \frac{L}{2\pi} \left[ \frac{4}{3} \text{Im} \ln \langle \Psi | e^{i\frac{2\pi x}{L}} | \Psi \rangle - \frac{1}{6} \text{Im} \ln \langle \Psi | e^{i\frac{4\pi x}{L}} | \Psi \rangle \right], \quad (\text{B3})$$

which is correct to  $\mathcal{O}(1/L^4)$ , as can be seen using the same type of reasoning as in Ref. 40. Eq. (B3) leads to a modified DBP polarization formula,

$$P_{\text{el}} = -\frac{e}{2\pi} \left[ \frac{4}{3} \text{Im} \ln \prod_{s=0}^{N-1} \det S(k_s, k_{s+1}) - \frac{1}{6} \text{Im} \ln \prod_{s=0}^{N-1} \det S(k_s, k_{s+2}) \right] + \mathcal{O}(1/L^4). \quad (\text{B4})$$

This is closely related to the expression obtained by combining Richardson's extrapolation, Eq. (20), with Eq. (B2), viewed as a finite-difference representation of the  $k$ -derivative in the continuum Berry-phase formula.<sup>41</sup>

We show in Figure 3 the convergence with the size  $N \times N \times N$  of the shifted Monkhorst-Pack grid of the second-order quantities  $\chi_{\infty}^{(2)}$ ,  $\alpha_{\text{TO}}$ , and  $\mu^{(2)}$  (these are the third derivatives of the electric enthalpy which involve at least one field derivative). For each quantity, we plot as a function of  $1/N^2$  the value obtained using both the conventional polarization expression (B2) (dashed line) and the modified expression (B4) (solid line). Notice that the values for  $\chi_{\infty}^{(2)}$ ,  $\alpha_{\text{TO}}$ , and  $\mu^{(2)}$  obtained from the former fall nearly on a straight line. Extrapolating to  $N = \infty$  through a least squares fit against  $1/N^2$  is a reliable way

of predicting the converged values, with errors of usually around 1%. This procedure requires several calculations at different  $N$ , starting at  $N = 12$  to avoid the contribution from higher-order terms in  $1/N$ . The modified polarization expression produces results of similar accuracy with a calculation for a single value of  $N$ . We found that  $N = 16$  usually provides accurate values for the calculation of nonlinear susceptibilities to within 1 pm/V. As we can see from the graph,  $\mu^{(2)}$  calculated in this way converges rapidly: The resulting value at  $N = 6$  is closer to the converged value of 0.284 nC/m than that calculated with the conventional functional at  $N = 20$ . The improvement for  $\alpha_{\text{TO}}$  and  $\chi_{\infty}^{(2)}$  is less dramatic, but

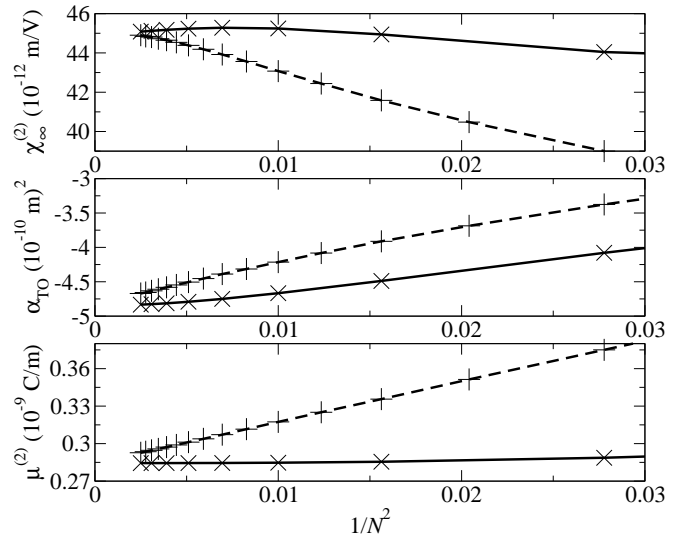


FIG. 3: Comparison of the convergence of  $\chi_{\infty}^{(2)}$ ,  $\alpha_{\text{TO}}$ , and  $\mu^{(2)}$  for AlP with respect to the  $k$ -point mesh when using the conventional discretized Berry-phase expression (B2) (dashed lines) versus using the modified expression (B4) (solid lines).

in general there is a clear improvement for most materials. The notable exception is GaAs, the material with the smallest gap, where there is an improvement for all quantities except  $\chi_{\infty}^{(2)}$ , which actually converges more slowly when using the modified fourth-order expression. We have found empirically that this expression works best for large band gap materials.

<sup>1</sup> W. L. Faust and C. H. Henry, Phys. Rev. Lett. **17**, 1265 (1966).

<sup>2</sup> A. Mayer and F. Keilmann, Phys. Rev. B **33**, 6954 (1986).

<sup>3</sup> G. Davies and E. Linfield, Physics World **17** (4), 37 (2004).

<sup>4</sup> A. Borak, Science **308**, 638 (2005).

<sup>5</sup> T. Dekorsy, V. A. Yakovlev, W. Seidel, M. Helm, and F. Keilmann, Phys. Rev. Lett. **90**, 055508 (2003).

<sup>6</sup> W. L. Faust, C. H. Henry, and R. H. Eick, Phys. Rev. **173**, 781 (1968).

<sup>7</sup> M. Barmentlo, G. W. 't Hooft, E. R. Eliel, E. W. M.

van der Ham, Q. H. F. Vrehen, A. F. G. van der Meer, and P. W. van Amersfoort, Phys. Rev. A **50**, R14 (1994).

<sup>8</sup> G. D. Boyd, T. J. Bridges, M. A. Pollack, and E. H. Turner, Phys. Rev. Lett. **26**, 387 (1971).

<sup>9</sup> M. A. Pollack and E. H. Turner, Phys. Rev. B **4**, 4578 (1971).

<sup>10</sup> C. Flytzanis, Phys. Rev. B **6**, 1264 (1972).

<sup>11</sup> D. A. Kleinman, Phys. Rev. **126**, 1977 (1962).

<sup>12</sup> R. C. Miller and W. A. Nordland, Phys. Rev. B **2**, 4896 (1970).



- <sup>13</sup> M. Cardona, F. Cerdeira, and T. A. Fjeldly, Phys. Rev. B **10**, 3433 (1974).
- <sup>14</sup> I. Souza, J. Íñiguez, and D. Vanderbilt, Phys. Rev. Lett. **89**, 117602 (2002).
- <sup>15</sup> A. Komornicki and J. W. McIver Jr., J. Chem. Phys. **70**, 2014 (1979).
- <sup>16</sup> K. Jackson, Phys. Stat. Sol. (b) **217**, 293 (2000).
- <sup>17</sup> X. Gonze *et al.*, Comput. Mater. Sci. **25**, 478 (2002).
- <sup>18</sup> J. P. Perdew, K. Burke, and M. Ernzerhof, Phys. Rev. Lett. **77**, 3865 (1996).
- <sup>19</sup> N. Troullier and J. L. Martins, Phys. Rev. B **43**, 1993 (1991).
- <sup>20</sup> B. Kirtman and B. Champagne, Int. Rev. Phys. Chem. **16**, 389 (1997).
- <sup>21</sup> R. D. King-Smith and D. Vanderbilt, Phys. Rev. B **47**, 1651 (1993).
- <sup>22</sup> D. Vanderbilt and R. Resta, in *Conceptual foundations of materials properties: A standard model for calculation of ground- and excited-state properties*, edited by S. G. Louie and M. L. Cohen (Elsevier, The Netherlands, 2006), p. 139.
- <sup>23</sup> M. Veithen, X. Gonze, and P. Ghosez, Phys. Rev. B **71**, 125107 (2005).
- <sup>24</sup> C. Flytzanis and J. Ducuing, Phys. Rev. **178**, 1218 (1968).
- <sup>25</sup> P. Y. Yu and M. Cardona, *Fundamentals of Semiconductors* (Springer, 2003), 3rd ed.
- <sup>26</sup> D. F. Nelson, ed., *Landolt-Bornstein* (Springer-Verlag, 2000), p. 324, New Series III/30B.
- <sup>27</sup> S. C. Varshney and A. A. Gundjian, J. Appl. Phys. **52**, 6301 (1981).
- <sup>28</sup> C. O. Rodriguez, R. A. Casali, E. L. Peltzer, O. M. Cappannini, and M. Methfessel, Phys. Rev. B **40**, 3975 (1989).
- <sup>29</sup> P. Gianozzi, S. de Gironcoli, P. Pavone, and S. Baroni, Phys. Rev. B **43**, 7231 (1991).
- <sup>30</sup> Z. H. Levine and D. C. Allan, Phys. Rev. B **44**, 12781 (1991).
- <sup>31</sup> A. Dal Corso, F. Mauri, and A. Rubio, Phys. Rev. B **53**, 15638 (1996).
- <sup>32</sup> C. Flytzanis, Phys. Lett. **34A**, 99 (1971).
- <sup>33</sup> C. Flytzanis, Phys. Rev. Lett. **29**, 772 (1972).
- <sup>34</sup> W. D. Johnston and I. P. Kaminow, Phys. Rev. **188**, 1209 (1969).
- <sup>35</sup> M. Cardona and G. Güntherodt, eds., *Light Scattering in Solids II*, vol. 50 of *Topics in Applied Physics* (Academic Press, 1982).
- <sup>36</sup> F. D. Martini, Phys. Rev. B **4**, 4556 (1971).
- <sup>37</sup> K. Rabe, cond-mat/0205655 (2002).
- <sup>38</sup> P. Umari and A. Pasquarello, Phys. Rev. B **68**, 085114 (2003).
- <sup>39</sup> R. Resta, Phys. Rev. Lett. **80**, 1800 (1998).
- <sup>40</sup> M. Stengel and N. A. Spaldin, Phys. Rev. B **73**, 075121 (2006).
- <sup>41</sup> J. Bennetto and D. Vanderbilt, Phys. Rev. B **53**, 15417 (1996).
- <sup>42</sup> The quantity  $\alpha_{\text{TO}}$  corresponds to  $\tilde{\alpha}^{(1)}$  of Refs. 32 and 10, and  $-\mathcal{P}$  of Refs. 13 and 27.